

IN-93  
JPL 773

## **Intergalactic Extinction of High Energy Gamma-Rays**

**F. W. Stecker  
Code 661, Laboratory for High Energy Astrophysics  
NASA Goddard Space Flight Center  
Greenbelt, MD 20771**



**National Aeronautics and Space Administration  
Goddard Space Flight Center  
Greenbelt, Maryland 20771**



# Intergalactic Extinction of High Energy Gamma-Rays <sup>★</sup>

F.W. Stecker

*Laboratory for High Energy Astrophysics, NASA Goddard Space Flight Center,  
Greenbelt, MD 20771, USA*

---

## Abstract

We discuss the determination of the intergalactic pair-production absorption coefficient as derived by Stecker and De Jager by making use of a new empirically based calculation of the spectral energy distribution of the intergalactic infrared radiation field as given by Malkan and Stecker. We show that the results of the Malkan and Stecker calculation agree well with recent data on the infrared background. We then show that Whipple observations of the flaring  $\gamma$ -ray spectrum of Mrk 421 hint at extragalactic absorption and that the HEGRA observations of the flaring spectrum of Mrk 501 appear to strongly indicate extragalactic absorption. We also discuss the determination of the  $\gamma$ -ray opacity at higher redshifts, following the treatment of Salamon and Stecker. We give a predicted spectrum, with absorption included for PKS 2155-304. This XBL lies at a redshift of 0.12, the highest redshift source yet observed at an energy above 0.3 TeV. This source should have its spectrum steepened by  $\sim 1$  in its spectral index between  $\sim 0.3$  and  $\sim 3$  TeV and should show an absorption cutoff above  $\sim 6$  TeV.

*Key words:* gamma-rays; BL Lac objects; gamma-ray bursts; background radiation; infrared

---

## 1 Introduction

Very high energy  $\gamma$ -ray beams from blazars can be used to measure the intergalactic infrared radiation field, since pair-production interactions of  $\gamma$ -rays with intergalactic IR photons will attenuate the high-energy ends of blazar spectra [1]. In recent years, this concept has been used successfully to place

---

<sup>★</sup> Invited Talk presented at the Workshop on TeV Astrophysics of Extragalactic Sources, Cambridge, MA, October 1998, to be published in the Proceedings.

upper limits on the the intergalactic IR field (IIRF) [2] - [6]. Determining the IIRF, in turn, allows us to model the evolution of the galaxies which produce it. As energy thresholds are lowered in both existing and planned ground-based air Cherenkov light detectors [7], cutoffs in the  $\gamma$ -ray spectra of more distant blazars are expected, owing to extinction by the IIRF. These can be used to explore the redshift dependence of the IIRF [8], [9].

There are now 66 grazars which have been detected by the *EGRET* team [11]. These sources, optically violent variable quasars and BL Lac objects, have been detected out to a redshift greater than 2. Of all of the blazars detected by *EGRET*, only the low-redshift BL Lac, Mrk 421 ( $z = 0.031$ ), has been seen by the Whipple telescope [12]. The fact that the Whipple team did not detect the much brighter *EGRET* source, 3C279, at TeV energies [13], [14] is consistent with the predictions of a cutoff for a source at its much higher redshift of 0.54 [1]. So too is the recent observation of three other very close BL Lacs ( $z < 0.05$ ), *viz.*, Mrk 501 ( $z = 0.034$ ) [15], 1ES2344+514 ( $z = 0.044$ ) [16], and PKS 2155-304 ( $z = 0.117$ ) [17] which were too faint at GeV energies to be seen by *EGRET*<sup>1</sup>.

## 2 The Opacity of Intergalactic Space to the IIRF

The formulae relevant to absorption calculations involving pair-production are given and discussed in Ref. [1]. For  $\gamma$ -rays in the TeV energy range, the pair-production cross section is maximized when the soft photon energy is in the infrared range:

$$\lambda(E_\gamma) \simeq \lambda_e \frac{E_\gamma}{2m_e c^2} = 2.4 E_{\gamma, \text{TeV}} \mu m \quad (1)$$

where  $\lambda_e = h/(m_e c)$  is the Compton wavelength of the electron. For a 1 TeV  $\gamma$ -ray, this corresponds to a soft photon having a wavelength near the K-band ( $2.2 \mu m$ ). (Pair-production interactions actually take place with photons over a range of wavelengths around the optimal value as determined by the energy dependence of the cross section; see eq. (6)).) If the emission spectrum of an extragalactic source extends beyond 20 TeV, then the extragalactic infrared field should cut off the *observed* spectrum between  $\sim 20$  GeV and  $\sim 20$  TeV, depending on the redshift of the source [8], [9].

---

<sup>1</sup> PKS 2155-304 was seen in one observing period by *EGRET* as reported in the Third EGRET Catalogue [11]

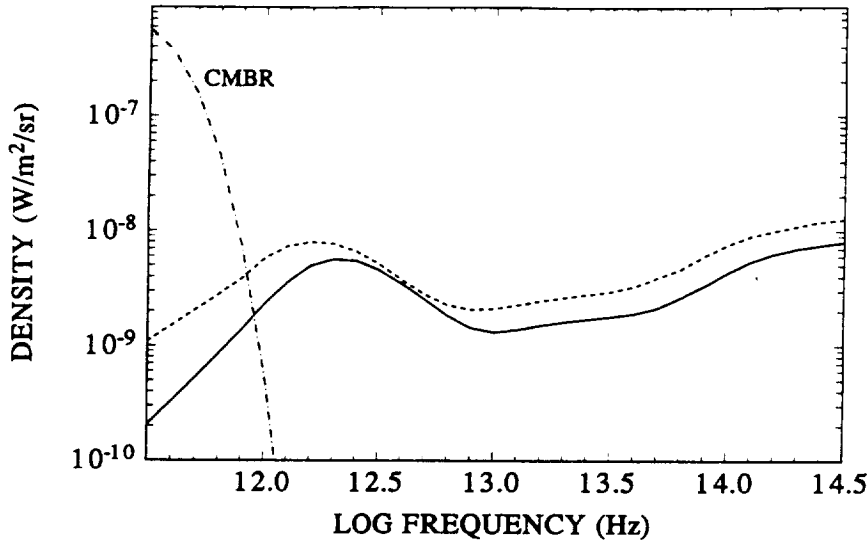


Fig. 1. The spectral energy distribution (SED) of the extragalactic IR radiation calculated by Malkan and Stecker [18] with the 2.7 K cosmic background radiation spectrum added. The solid line (lower IIRF curve) and the dashed line (higher IIRF curve) correspond to the middle and upper curves calculated by Malkan and Stecker with redshift-evolution assumptions as described in the text.

### 3 Absorption of Gamma-Rays at Low Redshifts

Stecker and De Jager [10] (hereafter SD98) have recalculated the absorption coefficient of intergalactic space using a new, empirically based calculation of the spectral energy distribution (SED) of intergalactic low energy photons by Malkan and Stecker [18] (hereafter MS98) obtained by integrating luminosity dependent infrared spectra of galaxies over their luminosity and redshift distributions. After giving their results on the  $\gamma$ -ray optical depth as a function of energy and redshift out to a redshift of 0.3, SD98 applied their calculations by comparing their results with the spectral data on Mrk 421 [19] and spectral data on Mrk 501 [20].

SD98 make the reasonable simplifying assumption that the IIRF is basically in place at a redshifts  $< 0.3$ , having been produced primarily at higher redshifts [8], [9], [21]. Therefore SD98 limited their calculations to  $z < 0.3$ . (The calculation of  $\gamma$ -ray opacity at higher redshifts [8],[9] will be discussed in the next section.)

SD98 assumed for the IIRF, two of the SEDs given in MS98 [18] (shown in Figure 1). The lower curve in Figure 1 (adapted from MS98) assumes evolution out to  $z = 1$ , whereas the upper curve assumes evolution out to  $z = 2$ . Evolution in stellar emissivity is expected to level off or decrease at redshifts greater than  $\sim 1.5$  [21]-[24] so that the two curves in Fig. 1 may be considered to be lower and upper limits, bounding the expected IR flux. Using these two SEDs for the IIRF, SD98 obtained parametric expressions for  $\tau(E, z)$  for  $z < 0.3$ , taking a Hubble constant of  $H_0 = 65 \text{ km s}^{-1} \text{ Mpc}^{-1}$  [30].

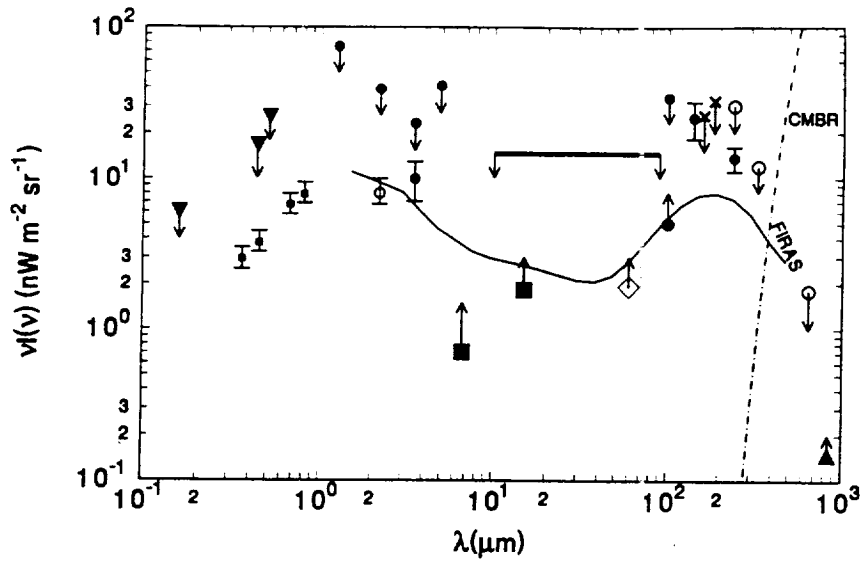


Fig. 2. The upper infrared SED from Malkan and Stecker compared with observational data and other constraints (courtesy O.C. De Jager).

The results of MS98 [18] generally agree well with very recent *COBE* data.<sup>2</sup> and with lower limits from galaxy counts and other considerations [25] - [29]. The results of MS are also in agreement with upper limits obtained from TeV  $\gamma$ -ray studies [2] - [6]. This agreement is illustrated in Figure 2 which shows the upper SED curve from MS98 in comparison with various data and limits.

The double-peaked form of the SED of the IIRF requires a 3rd order polynomial to approximate the opacity  $\tau$  in a parametric form. SD98 give the following approximation:

$$\log_{10}[\tau(E_{\text{TeV}}, z)] \simeq \sum_{i=0}^3 a_i(z) (\log_{10} E_{\text{TeV}})^i \text{ for } 1.0 < E_{\text{TeV}} < 50, \quad (2)$$

where the  $z$ -dependent coefficients are given by

$$a_i(z) = \sum_{j=0}^2 a_{ij} (\log_{10} z)^j. \quad (3)$$

Table 1 gives the numerical values for  $a_{ij}$ , with  $i = 0, 1, 2, 3$ , and  $j = 0, 1, 2$ . The numbers before the brackets are obtained using the lower IIRF SED shown in Figure 1; The numbers in the brackets are obtained using the higher IIRF SED. Equation (2) approximates  $\tau(E, z)$  to within 10% for all values of  $z$  and  $E$  considered.

<sup>2</sup> The derived *COBE* point at 140  $\mu\text{m}$  appears to be inconsistent with all calculated IIRF SEDs. It is also inconsistent with the spectrum of Mrk 501 (Konopelko, these proceedings), since it would imply a  $\gamma$ -ray optical depth  $\sim 6$  at 20 TeV.

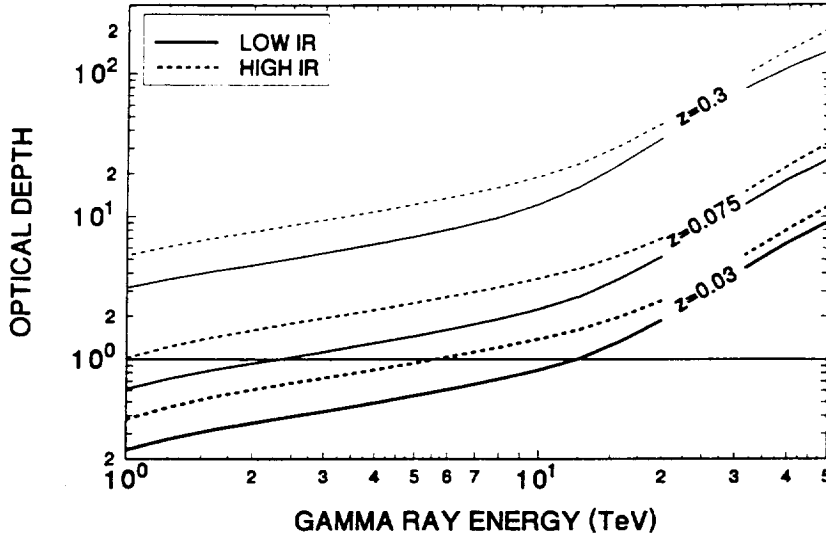


Fig. 3. Optical depth versus energy for  $\gamma$ -rays originating at various redshifts obtained using the SEDs corresponding to the lower IIRF (solid lines) and higher IIRF (dashed lines) levels shown in Fig. 1 (from SD98).

Table 1: Polynomial coefficients  $a_{ij}$

$j$	$a_{0j}$	$a_{1j}$	$a_{2j}$	$a_{3j}$
0	1.11(1.46)	-0.26( 0.10)	1.17(0.42)	-0.24( 0.07)
1	1.15(1.46)	-1.24(-1.03)	2.28(1.66)	-0.88(-0.56)
2	0.00(0.15)	-0.41(-0.35)	0.78(0.58)	-0.31(-0.20)

Figure 3 shows the results of the SD98 calculations of the optical depth for various energies and redshifts up to 0.3.

Figure 4 shows observed spectra for Mrk 421 [19] and Mrk 501 [20] in the flaring phase, compared with best-fit spectra of the form  $KE^{-\Gamma} \exp(-\tau(E, z = 0.03))$ , with  $\tau(E, z)$  given by the two appropriate curves shown in Figure 2. Because  $\tau < 1$  for  $E < 10$ , TeV, there is no obvious curvature in the *differential* spectra below this energy; rather, we obtain a slight steepening in the power-law spectra of the sources as a result of the weak absorption. This result implies that the *intrinsic* spectra of the sources should be harder by  $\delta\Gamma \sim 0.25$  in the lower IIRF case, and  $\sim 0.45$  in the higher IIRF case.

The SD98 results for the absorption coefficient as a function of energy do not differ dramatically from those obtained previously [31], [32]; however, they are more reliable because they are based on the empirically derived IIRF given by MS98, whereas all previous calculations of TeV  $\gamma$ -ray absorption were based

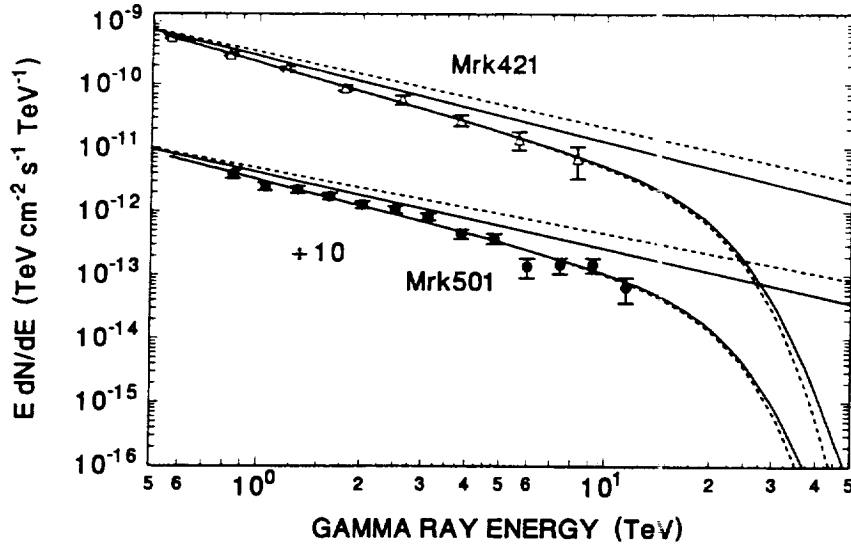


Fig. 4. The observed spectra of Mrk 421 (open triangles) [19] and Mrk 501 (solid circles - spectrum divided by 10) [20]. Best-fit absorbed spectra (of the form  $KE^{-\Gamma} \exp(-\tau(E, z = 0.03))$ ) and unabsorbed spectra ( $KE^{-\Gamma}$ ) for both sources are shown for  $\tau$  corresponding to the lower IIRF SED (solid lines;  $\Gamma = 2.36$  and  $2.2$  for Mrk 421 and Mrk 501 respectively) and higher IIRF SED (dashed lines;  $\Gamma = 2.2$  and  $2.03$  for Mrk 421 and Mrk 501 respectively) (from SD98).

on theoretical modeling of the IIRF. The MS98 calculation was based on data from nearly 3000 IRAS galaxies. These data included (1) the luminosity dependent infrared SEDs of galaxies, (2) the  $60\mu\text{m}$  luminosity function of galaxies and, (3) the redshift distribution of galaxies.

The SD98 calculations predict a significant intergalactic absorption effect which should cut off the spectra of Mrk 421 and Mrk 501 at energies greater than  $\sim 20$  TeV. Observations of these objects at large zenith angles, which give large effective threshold energies, may thus demonstrate the effect of intergalactic absorption. The observed spectrum of Mrk 501 in the flaring phase has now been extended to an energy of 24 TeV by observations of the *HEGRA* group. Their observations appear to strongly indicate the effect of extragalactic absorption as predicted by SD98 (see Konopelko, these proceedings).

Finally, we consider the source PKS 2155-304, an XBL located at a moderate redshift of 0.117, which has been reported by the Durham group to have a flux above 0.3 TeV of  $\sim 4 \times 10^{-11} \text{ cm}^{-2} \text{ s}^{-1}$  [17], close to that predicted by a simple SSC model [33]. Using the SD98 absorption results for the higher IR SED in Figure 1 and assuming an  $E^{-2}$  source spectrum, we predict an absorbed (observed) spectrum as shown in Figure 5. As indicated in the figure, we find that this source should have its spectrum steepened by  $\sim 1$  in its spectral index between  $\sim 0.3$  and  $\sim 3$  TeV and should show an absorption cutoff above  $\sim 6$  TeV.



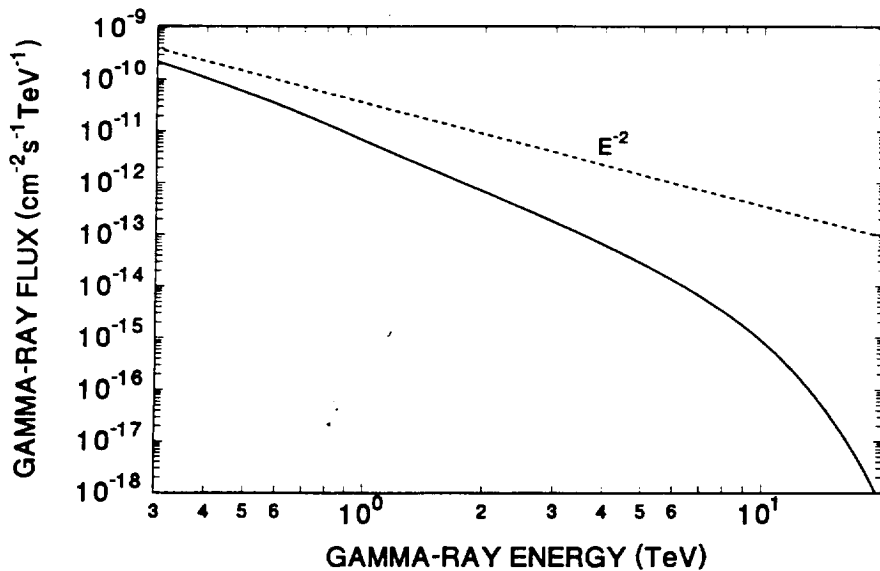


Fig. 5. Predicted differential absorbed spectrum, for PKS 2155-304 (solid line) assuming an  $E^{-2}$  source spectrum (dashed line).

#### 4 Absorption of Gamma-Rays at High Redshifts

We now discuss the absorption of 10 to 500 GeV  $\gamma$ -rays at high redshifts. In order to calculate such high-redshift absorption properly, it is necessary to determine the spectral distribution of the intergalactic low energy photon background radiation as a function of redshift as realistically as possible out to frequencies beyond the Lyman limit. This calculation, in turn, requires observationally based information on the evolution of the spectral energy distributions (SEDs) of IR through UV starlight from galaxies, particularly at high redshifts.

Conversely, observations of high-energy cutoffs in the  $\gamma$ -ray spectra of blazars as a function of redshift, which may enable one to separate out intergalactic absorption from redshift-independent cutoff effects, could add to our knowledge of galaxy formation and early galaxy evolution. In this regard, it should be noted that the study of blazar spectra in the 10 to 300 GeV range is one of the primary goals of a next generation space-based  $\gamma$ -ray telescope *GLAST* (*Gamma-ray Large Area Space Telescope*) (Ref. [34] and Gehrels, these proceedings) as well as *VERITAS* and other future ground based  $\gamma$ -ray telescopes.

Salamon and Stecker [9] (hereafter SS98) have calculated the  $\gamma$ -ray opacity as a function of both energy and redshift for redshifts as high as 3 by taking account

of the evolution of both the SED and emissivity of galaxies with redshift (see section 4.2). In order to accomplish this, they adopted the recent analysis of Fall, et al. [23] and also included the effects of metallicity evolution on galactic SEDs. They then gave predicted  $\gamma$ -ray spectra for selected blazars and extend our calculations of the extragalactic  $\gamma$ -ray background from blazars to an energy of 500 GeV with absorption effects included (see section 4.3). Their results indicate that the extragalactic  $\gamma$ -ray background spectrum from blazars should steepen significantly above 20 GeV, owing to extragalactic absorption. Future observations of a such a steepening would thus provide a test of the blazar origin hypothesis for the  $\gamma$ -ray background radiation. The results of the SS98 absorption calculations can be used to place limits on the redshifts of  $\gamma$ -ray bursts (see section 4.4). We describe and discuss these results in the following subsections.

#### *4.1 Redshift Dependence of the Intergalactic Low Energy SED*

The opacity of intergalactic space to high energy  $\gamma$ -rays as a function of redshift depends upon the number density of soft target photons (IR to UV) as a function of redshift, photons whose production is dominated by stellar emission. To evaluate the SED of the IR-UV intergalactic radiation field we must integrate the total stellar emissivity over time. This requires an estimate of the dependence of stellar emissivity on redshift. Previous calculations of  $\gamma$ -ray opacity have either assumed that essentially all of the background was in place at high redshifts, corresponding to a burst of star formation at the initial redshift [35], [36], [31] or strong evolution [37], or that there is no evolution [37].

Pei and Fall [38] have devised a method for calculating stellar emissivity which bypasses the uncertainties associated with estimates of poorly defined luminosity distributions of evolving galaxies. The core idea of their approach is to relate the star formation rate directly to the evolution of the neutral gas density in damped Ly  $\alpha$  systems, and then to use stellar population synthesis models to estimate the mean co-moving stellar emissivity  $\mathcal{E}_\nu(z)$  of the universe as a function of frequency  $\nu$  and redshift  $z$  [23]. The SS98 calculation of stellar emissivity closely follows this elegant analysis, with minor modifications.

Damped Ly  $\alpha$  systems are high-redshift clouds of gas whose neutral hydrogen surface density is large enough ( $> 2 \times 10^{20} \text{ cm}^{-2}$ ) to generate saturated Ly  $\alpha$  absorption lines in the spectra of background quasars that happen to lie along and behind common lines of sight to these clouds. These gas systems are believed to be either precursors to galaxies or young galaxies themselves, since their neutral hydrogen (HI) surface densities are comparable to those of spiral galaxies today, and their co-moving number densities are consistent

with those of present-day galaxies [39], [40]. It is in these systems that initial star formation presumably took place, so there is a relationship between the mass content of stars and of gas in these clouds; if there is no infall or outflow of gas in these systems, the systems are “closed”, so that the formation of stars must be accompanied by a reduction in the neutral gas content. Such a variation in the HI surface densities of Ly  $\alpha$  systems with redshift is seen, and is used by Pei and Fall [38] to estimate the mean cosmological rate of star formation back to redshifts as large as  $z = 5$ .

Pei and Fall [38] estimated the neutral (HI plus HeI) co-moving gas density  $\rho_c \Omega_g(z)$  in damped Ly  $\alpha$  systems from observations of the redshift evolution of these systems by Lanzetta, et al. [41]. Lanzetta, et al. have observed that while the number density of damped Ly  $\alpha$  systems appears to be relatively constant over redshift, the fraction of higher density absorption systems within this class of objects decreases steadily with decreasing redshift. They attribute this to a reduction in gas density with time, roughly of the form  $\Omega_g(z) = \Omega_{g0} e^z$ , where  $\rho_c \Omega_{g0}$  is the current gas density in galaxies. Pei and Fall have taken account of self-biasing effects to obtain a corrected value of  $\Omega_g(z)$ . SS98 [9] have reproduced their calculations to obtain  $\Omega_g(z)$  under the assumptions that the asymptotic, high redshift value of the neutral gas mass density is  $\Omega_{g,i} = 1.6 \times 10^{-2} h_0^{-1}$ , where  $h_0 \equiv H_0/(100 \text{ km s}^{-1} \text{ Mpc}^{-1})$ . In a “closed galaxy” model, the change in co-moving stellar mass density  $\rho_c \dot{\Omega}_s(z) = -\rho_c \dot{\Omega}_g(z)$ , since the gas mass density  $\rho_c \Omega_g(z)$  is being converted into stars. This determines the star formation rate and consequent stellar emissivity. The rate of metal production,  $\dot{Z}$ , is related to star formation rate by  $\Omega_g \dot{Z} = \zeta \dot{\Omega}_s$ , where  $\zeta = 0.38 Z_\odot$  is the metallicity yield averaged over the initial stellar mass function, with  $Z_\odot$  being the solar metallicity [38]. This gives a metallicity evolution  $Z(z) = -\zeta \ln[\Omega_g(z)/\Omega_{g,i}]$ .

In order to determine the mean stellar emissivity from the star formation rate, an initial mass function (IMF)  $\phi(M)$  must be assumed for the distribution of stellar masses  $M$  in a freshly synthesized stellar population. To further specify the luminosities of these stars as a function of mass  $M$  and age  $T$ , Fall, Charlot, and Pei [23] use the Bruzual-Charlot (BC) population synthesis models for the spectral evolution of stellar populations [42], [43]. In these population synthesis models, the specific luminosity  $L_{\text{star}}(\nu, M, T)$ , of a star of mass  $M$  and age  $T$  is integrated over a specified IMF to obtain a total specific luminosity  $S_\nu(T)$  per unit mass for an entire population, in which all stellar members are produced simultaneously ( $T = 0$ ). Following Fall, Charlot, and Pei [23], SS98 used the BC model corresponding to a Salpeter IMF,  $\phi(M) dM \propto M^{-2.35} dM$ , where  $0.1 M_\odot < M < 125 M_\odot$ . The mean co-moving emissivity  $\mathcal{E}_\nu(t)$  was then obtained by convolving over time  $t$  the specific luminosity with the mean co-moving mass rate of star formation. SS98 also obtained metallicity correction factors for stellar radiation at various wavelengths. Increased metallicity gives a redder population spectrum [44], [45].

SS98 calculated stellar emissivity as a function of redshift at 0.28  $\mu\text{m}$ , 0.44  $\mu\text{m}$ , and 1.00  $\mu\text{m}$ , both with and without a metallicity correction. They agree well with the emissivity obtained by the Canada-French Redshift Survey [46] over the redshift range of the observations ( $z \leq 1$ ).

The stellar emissivity in the universe is found to peak at  $1 \leq z \leq 2$ , dropping off steeply at lower redshifts and more slowly at higher redshifts. Indeed, Madau, et al. [21] have used observational data from the Hubble Deep Field to show that metal production has a similar redshift distribution, such production being a direct measure of the star formation rate. (See also Ref. [24]).

The co-moving radiation energy density  $u_\nu(z)$  is the time integral of the co-moving emissivity  $\mathcal{E}_\nu(z)$ ,

$$u_\nu(z) = \int_z^{z_{\max}} dz' \mathcal{E}_{\nu'}(z') \frac{dt}{dz}(z') e^{-\tau_{\text{eff}}(\nu, z, z')}, \quad (4)$$

where  $\nu' = \nu(1 + z')/(1 + z)$  and  $z_{\max}$  is the redshift corresponding to initial galaxy formation. The extinction term  $e^{-\tau_{\text{eff}}}$  accounts for the absorption of ionizing photons by the clumpy intergalactic medium (IGM) that lies between the source and observer. Although the IGM is effectively transparent to non-ionizing photons, the absorption of photons by HI, HeI and HeII can be considerable [47].

#### 4.2 The Gamma-Ray Opacity at High Redshifts

With the co-moving energy density  $u_\nu(z)$  evaluated [9] (SS98), the optical depth for  $\gamma$ -rays owing to electron-positron pair production interactions with photons of the stellar radiation background can be determined from the expression [1]

$$\tau(E_0, z_e) = c \int_0^{z_e} dz \frac{dt}{dz} \int_0^2 dx \frac{x}{2} \int_0^\infty d\nu (1 + z)^3 \left[ \frac{u_\nu(z)}{h\nu} \right] \sigma_{\gamma\gamma}(s) \quad (5)$$

where  $s = 2E_0 h\nu x(1 + z)$ ,  $E_0$  is the observed  $\gamma$ -ray energy at redshift zero,  $\nu$  is the frequency at redshift  $z$ ,  $z_e$  is the redshift of the  $\gamma$ -ray source,  $x = (1 - \cos \theta)$ ,  $\theta$  being the angle between the  $\gamma$ -ray and the soft background photon,  $h$  is Planck's constant, and the pair production cross section  $\sigma_{\gamma\gamma}$  is zero for center-of-mass energy  $\sqrt{s} < 2m_e c^2$ ,  $m_e$  being the electron mass. Above this threshold,

$$\sigma_{\gamma\gamma}(s) = \frac{3}{16} \sigma_T (1 - \beta^2) \left[ 2\beta(\beta^2 - 2) + (3 - \beta^4) \ln \left( \frac{1 + \beta}{1 - \beta} \right) \right], \quad (6)$$

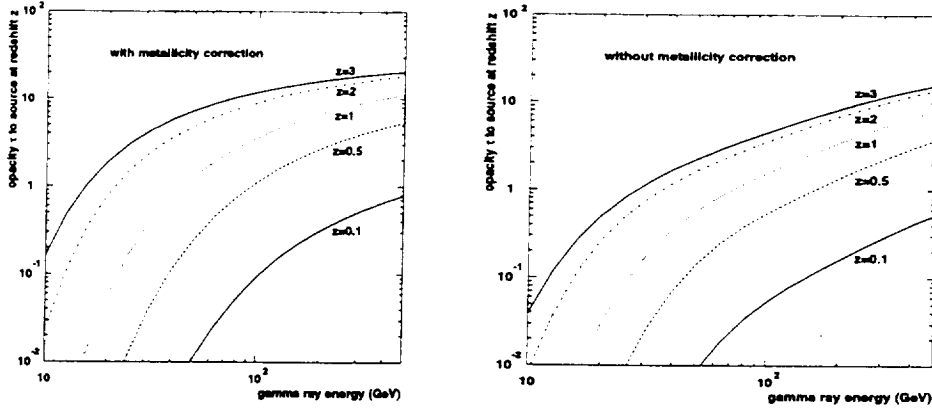


Fig. 6. The opacity  $\tau$  of the universal soft photon background to  $\gamma$ -rays as a function of  $\gamma$ -ray energy and source redshift (from SS98) [9]. These curves are calculated with and without a metallicity correction.

where  $\beta = (1 - 4m_e^2 c^4/s)^{1/2}$ .

Figure 6 shows the opacity  $\tau(E_0, z)$  for the energy range 10 to 500 GeV, calculated by SD98 both with and without a metallicity correction. Extinction of  $\gamma$ -rays is negligible below 10 GeV.

The weak redshift dependence of the opacity at the higher redshifts as shown in Figure 6 indicates that the opacity is not very sensitive to the initial epoch of galaxy formation, contrary to the speculation of MacMinn and Primack [31]. In fact, the uncertainty in the metallicity correction (see Figure 6) would obscure any dependence on  $z_{max}$  even further.

#### 4.3 The Effect of Absorption on the Spectra of Blazars and the Gamma-Ray Background

With the  $\gamma$ -ray opacity  $\tau(E_0, z)$  calculated out to  $z = 3$ , the cutoffs in blazar  $\gamma$ -ray spectra caused by extragalactic pair production interactions with stellar photons can be predicted. The left graph in Figure 7 from Ref. [9] (SS98) shows the effect of the intergalactic radiation background on a few of the  $\gamma$ -ray blazars (“grazars”) observed by *EGRET*, viz., 1633+382, 3C279, 3C273, and Mrk 421, assuming that the mean spectral indices obtained for these sources by *EGRET* extrapolate out to higher energies attenuated only by intergalactic absorption. Observed cutoffs in grazar spectra may be intrinsic cutoffs in  $\gamma$ -ray production in the source, or may be caused by intrinsic  $\gamma$ -ray absorption within the source itself.

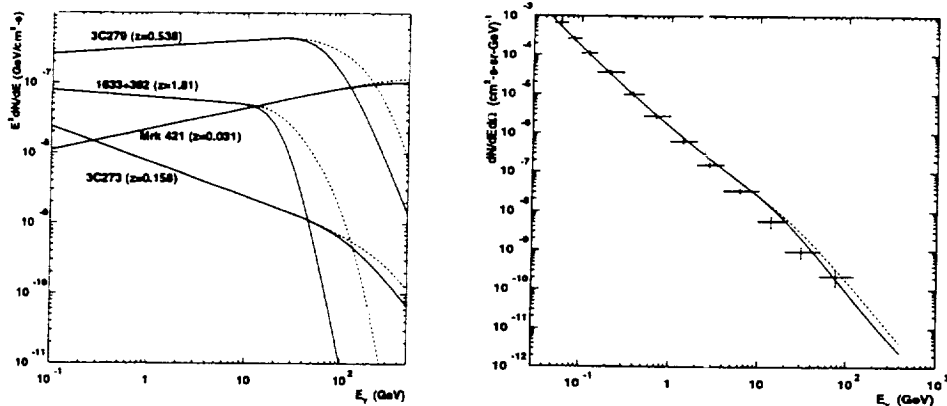


Fig. 7. The left graph shows the effect of intergalactic absorption by pair-production on the power-law spectra of four prominent grazars: 1633+382 ( $z = 1.81$ ), 3C279 ( $z = 0.54$ ), 3C273 ( $z = 0.15$ ), and Mrk 421 ( $z = 0.031$ ); The right graph shows the extragalactic  $\gamma$ -ray background spectrum predicted by the unresolved blazar model of Ref. [48] with absorption included, calculated for a mean *EGRET* point-source sensitivity of  $10^{-7} \text{ cm}^{-2}\text{s}^{-1}$ , compared with the *EGRET* data on the  $\gamma$ -ray background [49]. The solid (dashed) curves are calculated with (without) the metallicity correction function (from SS98 [9]).

The right hand graph in Figure 7 shows the background spectrum predicted from unresolved blazars [48], [9] compared with the *EGRET* data [49]. Note that the spectrum steepens above 20 GeV, owing to extragalactic absorption by pair-production interactions with radiation from external galaxies, particularly at high redshifts. Above 10 GeV, blazars may have natural cutoffs in their source spectra [33] and intrinsic absorption may also be important in some sources [50]. Thus, above 10 GeV the calculated background flux from unresolved blazars shown in Figure 7 may actually be an upper limit. Whether cutoffs in grazar spectra are primarily caused by intergalactic absorption can be determined by observing whether the grazar cutoff energies have the type of redshift dependence predicted here.

#### 4.4 Constraints on Gamma-ray Bursts

The discovery of optical and X-ray afterglows of  $\gamma$ -ray bursts and the identification of host galaxies with measured redshifts, *i.e.*, [51], [52], has lead the accumulation of evidence that these bursts are highly relativistic fireballs originating at cosmological distances [53] and may be associated primarily with early star formation [54].

As indicated in Figure 6  $\gamma$ -rays above an energy of  $\sim 15$  GeV will be attenuated if they are emitted at a redshift of  $\sim 3$ . On 17 February 1994, the *EGRET* telescope observed a  $\gamma$ -ray burst which contained a photon of energy  $\sim 20$  GeV

[55]. If one adopts the opacity results which include the metallicity correction, the highest energy photon in this burst would be constrained to most likely have originated at a redshift less than  $\sim 2$ . Future detectors such as *GLAST* (Ref. [34], also Gehrels, these proceedings) may be able to place better redshift constraints on bursts observed at higher energies. Such constraints may further help to identify the host galaxies of  $\gamma$ -ray bursts.

## 5 Appendix: Elegy to an AGN Gamma-Ray

*Cast off from a dimly distant shore,  
 Thrown upon thy longtime voyage hence,  
 Whilst smote upon thy way, in combat doubly charged,  
 Of thy brave companions, the highest born  
 Be now vanished from amongst the world.  
 Lest ye fear that they be anon forgot,  
 I pause here, their ordained fate to fast relate,*

*That all about may list and mark me well,  
 For their absence doth their final doom well tell.*

## 6 Acknowledgment

I wish to acknowledge that the work presented here was a result of extensive collaboration with O.C. De Jager, M.A. Malkan, and M.H. Salamon, as indicated in the references cited. I also wish to thank Okkie De Jager for helping with the manuscript.

## References

- [1] F. W. Stecker, O.C. De Jager and M.H. Salamon *Astrophys. J. (Lett.)* 390 (1992) L49.
- [2] F.W. Stecker, O.C. De Jager, *Astrophys. J. (Lett.)* 415 (1993) L71.
- [3] E. Dwek, J. Slavin, *Astrophys. J.* 436 (1994) 696.
- [4] F.W. Stecker, O.C. De Jager, in *Proc. Kruger National Park Conference on TeV Gamma Ray Astrophysics, Berg-en-Dal, South Africa* ed. O.C. De Jager (1998) p. 39.

- [5] T. Stanev, A. Franceschini, *Astrophys. J. (Lett.)* 494 (1998) L159.
- [6] S. Biller, et al. , *Phys. Rev. Letters* 80 (1998) 2992.
- [7] O.C. De Jager, *Proc. Kruger National Park Conference on TeV Gamma Ray Astrophysics, Berg-en-Dal, South Africa* (1998).
- [8] F.W. Stecker, M.H. Salamon, *Proc. 25th Internat. Cosmic Ray Conf. , Durban 3* (1997) 317.
- [9] M.H. Salamon, F.W.Stecker, *Astrophys. J.* 493 (1998) 547 (SS98).
- [10] F.W. Stecker, O.C. De Jager, *Astron. and Astr.* 334 (1998) L85 (SD98).
- [11] Hartman, R.C., et al. , *Astrophys. J. Suppl.*, (1999) in press.
- [12] M. Punch, et al. , *Nature* 358 (1992) 477.
- [13] G. Vacanti, et al. , *Proc. 21st Internat. Cosmic Ray Conf. 2* (1990) 329.
- [14] Kerrick, A.D. et al. , *Proc. 23rd Int'l. Cosmic Ray Conf., U. Calgary Press, Calgary, 1* (1993) 405.
- [15] J. Quinn, et al. , *Astrophys. J. (Lett.)* 456 (1996) L83.  
3 (1997) 277.
- [16] M. Catanese, et al. , *Astrophys. J.* 501 (1998) 616.
- [17] P.M. Chadwick, et al. , e-print astro-ph/9810209, *Astrophys. J.*, in press (see also these proceedings).
- [18] M.A. Malkan and F.W. Stecker, *Astrophys. J.* 496 (1998) 13 (MS98).
- [19] J.E. McEnery, et al. , *Proc. 25th Internat. Cosmic Ray Conf. , Durban 3* (1997) 257.
- [20] F. Aharonian, et al. , *Astron. and Astr.* 327 (1997) L5.
- [21] P. Madau, P. 1996, in *Star Formation Near and Far*, ed. S.S. Holt and L.G. Mundy, *AIP Symp. Proc. No. 393* (New York: Amer. Inst. Phys.), 481.
- [22] E. Bertin, M. Dennefeld and M. Moshir, *Astron. and Astr.* 323 (1997) 685.
- [23] S.M. Fall, S. Charlot and Y.C. Pei, *Astrophys. J. (Lett.)* , 464 (1996) L43.
- [24] C.C. Steidel, et al. , e-print astro-ph/9812167.
- [25] J.L. Puget, et al. , *Astron. and Astr.* 308, L5.
- [26] M. G. Hauser, et al. , *Astrophys. J.* 508 (1998) 25.
- [27] E. Dwek, et al. , *Astrophys. J.* 508 (1998) 106.
- [28] D.J. Fixen, et al. *Astrophys. J.* 508 (1998) 123.
- [29] E. Dwek, R.G. Arendt, *Astrophys. J.* 508 (1998) L9.



- [30] R.G. Gratton, et al. , Publ. Astr. Soc. Pac. 402 (1997) 651.
- [31] D. MacMinn, J.R. Primack, Space Sci. Rev. 75 (1996) 413.
- [32] F.W. Stecker, O.C. De Jager, Astrophys. J. 476 (1997) 712.
- [33] F.W. Stecker, O.C. De Jager, M.H. Salamon, M.H., Astrophys. J. (Lett.) 473 (1996) L75.
- [34] E.D. Bloom, E.D., Space Sci. Rev. 75 (1996) 109.
- [35] F.W. Stecker *Unveiling the Cosmic Infrared Background (AIP Conf. Proc. 348)*, (Amer. Inst. of Physics, New York), p. 181 (1996).
- [36] F.W. Stecker, O.C. de Jager, Space Sci. Rev., 75 (1996) 413.
- [37] P. Madau, E.S. Phinney, Astrophys. J. 456 (1996) 124.
- [38] Y.C. Pei, S.M. Fall, Astrophys. J. 454 (1995) 69.
- [39] A.M. Wolfe, Phil. Trans. Royal Soc. London, A, 320 (1986) 503.
- [40] M. Pettini M., et al. , Astrophys. J. 426 (1994) 79.
- [41] K.M. Lanzetta, A.M. Wolfe, D.A. Turnshek, D.A., Astrophys. J., 440 (1995) 435.
- [42] A.G. Bruzual, S. Charlot, S., Astrophys. J. 405 (1993) 538.
- [43] S. Charlot, A.G. Bruzual A.,G., Astrophys. J. 457 (1991) 625.
- [44] G. Worthey, Astrophys. J. Supp. 95 (1994) 107.
- [45] G. Bertelli, et al. , Astron. and Astr. Suppl. 106 (1994) 275.
- [46] S.J. Lilly, et al. , Astrophys. J. (Lett.) 460 (1996) L1.
- [47] P. Madau, Astrophys. J. 441 (1995) 18.
- [48] F.W. Stecker, M.H. Salamon, Astrophys. J. 464 (1996) 600.
- [49] P. Sreekumar, et al. , Astrophys. J. 494 (1998) 523.
- [50] R. Protheroe, P.L. Biermann, Astropart. Phys. 6 (1996) 45.
- [51] M. Metzger, et al. , Nature 387 (1997) 878.
- [52] S.R. Kulkarni, et al. , Nature 393 (1998) 35.
- [53] M. Livio, et al. , Proc. 4th Huntsville Symp. on Gamma Ray Bursts, ed. C.A. Meegan, et al. , (New York: Amer. Inst. Phys.) p. 483 (1998).
- [54] S.G. Djorgovski, S.R. Kulkarni, J.S. Bloom, e-print astro-ph/9808188.
- [55] K. Hurley, et al. , Nature, 372 (1994) 652.

